

# Polymerization of Acrylonitrile Using Magnetron Deposition Technique

V. S. SHIRODKAR,<sup>1</sup> R. T. JATHAR,<sup>1</sup> A. M. BAPAT,<sup>1</sup> S. D. KULKARNI,<sup>2</sup> and N. V. BHAT<sup>2</sup>

<sup>1</sup>Solid-State Electronic Lab, The Institute of Science, 15 Madame Cama Road, Bombay 400 032, and <sup>2</sup>Physics Section, Centre of Advance Studies, Department of Chemical Technology, Matunga, Bombay 400 019, India

## SYNOPSIS

Polymerization of acrylonitrile (PAN) in a capacitively coupled glow discharge under magnetic enhancement was studied. The design aspects of a magnetron electrode and its characteristics are described. The study suggests that an improved magnetron design helps in achieving a higher monomer conversion ratio that improves the quality of films and allows the use of lower system pressure. Thin, uniform, pinhole free films of PAN having very high molecular weight were formed. © 1994 John Wiley & Sons, Inc.

## INTRODUCTION

In recent years plasma polymerization has assumed considerable technological importance. The technique of plasma polymerization has been investigated by many.<sup>1-6</sup> Polymerization of acetylene, ethylene, styrene, and other monomers has been accomplished. Yasuda discussed in detail the effect of various parameters of reaction chamber and electrode assemblies. The effect of rate of flow, chamber pressure, power, interelectrode separation etc. have also been investigated in detail.<sup>7-9</sup>

The main drawback of the reaction chamber, where the plasma is generated using radio frequency (rf) or dc voltage, is that the plasma tends to spread throughout the volume of the chamber and the deposition occurs not only on the substrate but also on the walls of the chamber, supports, and other components. This is undesirable because these depositions contaminate the assembly, giving rise to some undesirable products in subsequent runs and material loss. For any industrial application it is desirable that the process involve minimal monomer loss, lower power requirement, and improvement in the quality of films. To accomplish these goals, it is therefore necessary to confine the plasma in the chamber, particularly in the interelectrode gap using a magnetic field.

An electrode arrangement involving a superimposed magnetic field is generally termed a magnetron. Magnetron electrodes effectively confine plasma to a small region of electrodes, thereby requiring a smaller volume of monomer. In addition the deposition can be realized at a much lower chamber pressure, on the order of a few tens of mTorr. The energy input to the reacting species is generally expressed by  $W/FM$  ratio where  $W$  is the rf power in watts,  $F$  the flow rate, and  $M$  the molecular weight of monomer. The use of a magnetron enables the delivery of higher rf power to the reacting species by virtue of lower  $FM$ .

Therefore, in this article we describe the use of a modified magnetron electrode to polymerize acrylonitrile (AN). However, plasma polymerization of AN without magnetic enhancement has been reported by Hirai,<sup>10</sup> Jaquemin,<sup>11</sup> and Brodure.<sup>12</sup>

## EXPERIMENTAL

The magnetron assembly used for the polymerization of AN is depicted in Figure 1. It consisted of a cylindrical cathode and a disc-shaped anode, each of 75-mm diameter. Two magnets, one ring shaped with ID and OD of 40 and 75 mm, respectively, and another cylindrical in shape, 10-mm diameter, were used. These magnets were housed with an aluminum spacer in the cavity of the cathode. The polarities of the magnets were arranged to obtain a rel-

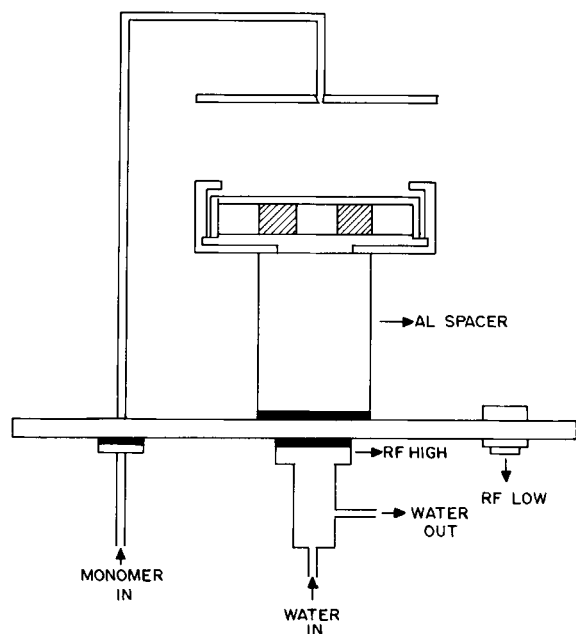


**Figure 1** Schematic diagram of magnetron used for polymerization of acrylonitrile.

atively uniform magnetic field over the cathode region. The cathode had a provision to circulate chilled water in its cavity to cool the magnets during the polymerization. The edges of the cathode and the anode were suitably rounded to eliminate the edge effect. A grounded aluminium shield of proper shape was provided to the cathode, positioned in cathode dark space. The Anode was made of a disc of SS 316 material with a small opening at its centre to introduce the monomer and could be moved along the vertical axis to change the distance between the electrodes. The entire assembly was mounted on the base plate of vacuum system using feedthroughs. The anode was grounded through the base plate and the cathode was isolated from it.

The chamber was evacuated using an oil diffusion pump backed by a mechanical pump. The mechanical pump was fitted with an oil mist filter that prevented any oil vapours from entering the chamber. A liquid nitrogen trap was also introduced between the diffusion pump and the quarterswing baffle valve (QSB). The QSB was used for gas throttling to obtain desired steady pressure in the work chamber during polymerization. The chamber pressure was monitored using a digital pirani gauge. The flow rate of AN vapours was monitored using mass flow controllers, supplied by Unit Instruments (California, USA), model URS-100-5 with UFC-1100, calibrated for the given gas. The rf power was delivered using an RFA 1000 supplied by RF Applications Ltd. (Sussex, UK) and fitted with meters to read input power and reflected power.

The rf power supply, operated at 13.56 MHz, was able to deliver continuously variable power from 0 to 1000 W. An autotuned impedance matching network, interposed between the rf supply and the electrode, could automatically maintain reflected power to the minimum.

The substrates used for the study included carefully cleaned glass slides, and plates of stainless steel, copper, and aluminium. These were treated for 30 min in argon gas plasma, prior to polymer deposition, to clean the surface. The chamber was evacuated to  $10^{-5}$  Torr and argon gas was flushed. When the pressure dropped to  $2 \times 10^{-2}$  Torr plasma was created for substrate cleaning. After the plasma cleaning, the flow of argon gas was shut off and AN vapours were introduced. A flow of monomer gas and QSB were adjusted to give a steady pressure of  $5 \times 10^{-2}$  Torr in the chamber. It was found that when plasma was initiated the pressure dropped; but as far as possible, efforts were made to maintain it around  $5 \times 10^{-2}$  Torr. The film thickness was measured using an interferometric technique and a Dektak surface profilometer.

## RESULTS AND DISCUSSION

### Distribution and Effect of Magnetic Field

Figure 2 gives the distribution of the parallel and perpendicular components of the magnetic field at the surface of the cathode. In this case the component of the magnetic field parallel to the electric field, that is, along the axis of the electrodes, is con-

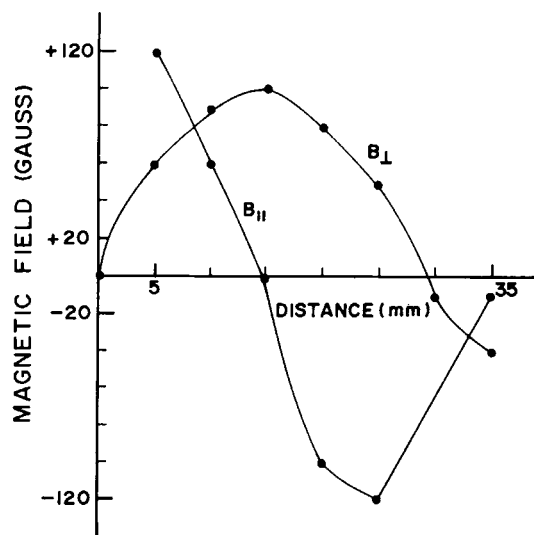


**Figure 2** Distribution, parallel ( $B_{||}$ ) and perpendicular ( $B_{\perp}$ ), of magnetic field along the magnetron surface.

sidered as  $B_{11}$  and the one perpendicular to it is termed  $B_1$ . It is seen that the  $B_{11}$  vanishes near the aluminium spacer introduced between the magnets and the  $B_1$  reaches the maximum. The films deposition occurring in this region showed that the deposited material turns slightly brownish in colour possibly due to the bombardment of energetic electrons confined in the region. However, the thickness of the film was found to be uniform in the entire region of the magnetron surface.

### Conditions of Polymerization

The polymerization was carried out by varying a few parameters of the reactor chamber. This was done in order to find the optimum conditions that would give the best films.

### Distance Between Electrodes

The distance between the two electrodes was varied from 1–4 cm. The rates of depositions in each case are plotted as rate versus distance and is depicted in Figure 3. It can be seen that as the distance between the electrodes increases the rate of deposition decreases. This behaviour can be understood as a decrease in the interelectrode distance yielding a higher ratio of power to volume ( $W/FM$ ). However, at distances less than 1 cm, it was found that, although the rates are higher, the quality of the film

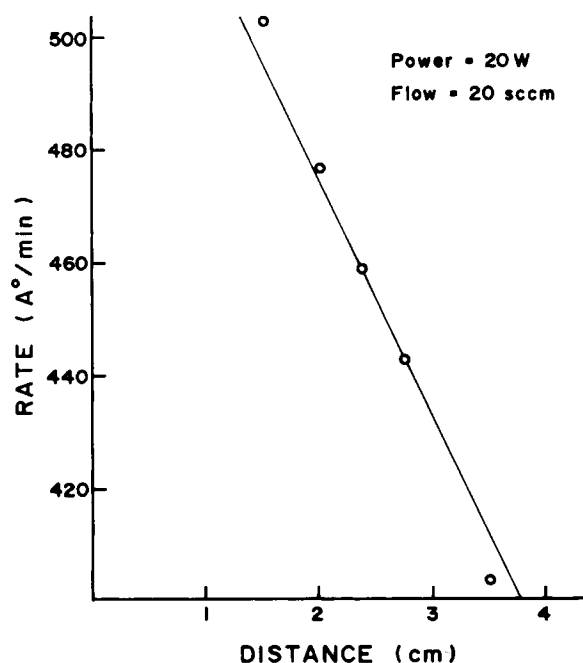


**Figure 3** Rate of deposition as a function of interelectrode distance.

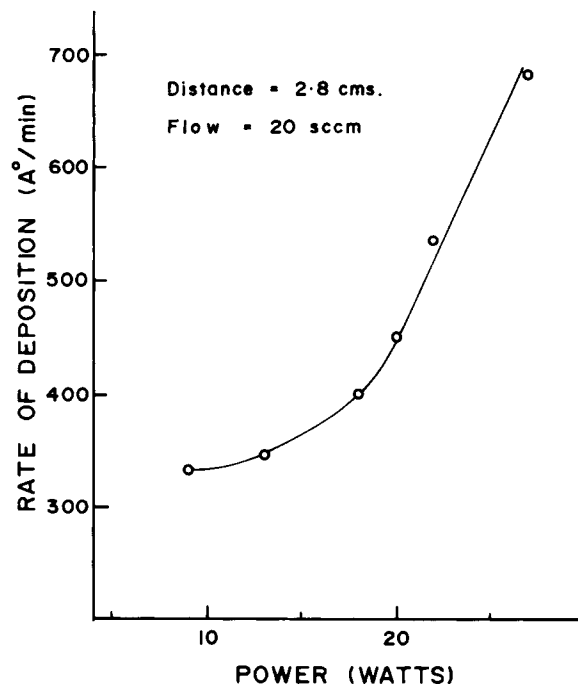


**Figure 4** A plot of deposition rate versus power for fixed interelectrode distance of 2.8 cm and monomer flow rate of 20 sccm.

is not good. The film became brownish, possibly due to heavy bombardment of ions and heating. The best quality of film could be obtained at a distance of 2.8 cm. At various distances it was found that, apart from the lower deposition rate, the films were not continuous; they had a grainy appearance. In the subsequent experiments, therefore, the distance of 2.8 cm was kept constant.

### Power

The power applied has an enhancement effect on the rate of deposition as well as quality of the films. In Figure 4 is shown the dependence of the rate of deposition with power for a fixed interelectrode distance of 2.8 cm. It may be seen that the rate of deposition increases slowly in the beginning and then increases rapidly at power greater than 18 W. This is due to the fact that for very low powers sufficient ionisation is not effected. With a further increase in power the rate of deposition increases linearly with increasing power. Qualitatively it was observed that the best transparent films were obtained at a power of 20–24 W.

### Flow Rate of Monomer

It is well established in the case of other monomers like styrene<sup>13</sup> etc. that the rate of deposition depends

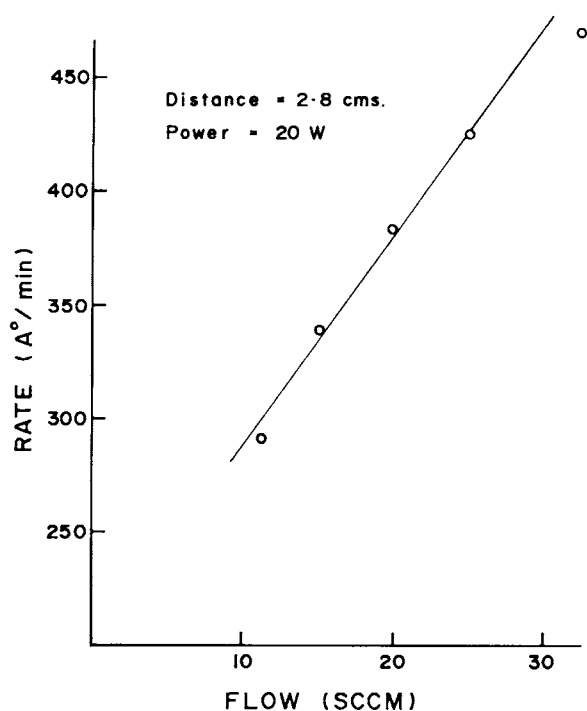


**Figure 5** Rate of deposition as a function of rate of flow of acrylonitrile.

on the rate of flow. It may be seen from Figure 5, that in the case of AN the rate of deposition increases linearly with the flow rate of monomer. Best

quality films were obtained at the flow rate of 20 sccm.

### Characterization

Infrared absorption of plasma polymerized acrylonitrile (PAN) was recorded using Perkin-Elmer FTIR. The spectra corresponding to chemically polymerized, cPAN, and plasma polymerized, pPAN, are shown in Figure 6. Typical characteristics of the absorption band for cPAN at  $2250\text{ cm}^{-1}$  corresponding to  $\text{C}\equiv\text{N}$  as well as an absorption band at  $1620\text{ cm}^{-1}$  corresponding to  $\text{C}=\text{N}$  are clearly visible.<sup>14,15</sup> In addition the spectrum for cPAN shows strong absorption peaks at  $2950\text{ cm}^{-1}$  ( $\text{C}-\text{H}$  stretching),  $1460\text{ cm}^{-1}$  ( $\text{C}-\text{H}$  bending),  $1360-1390\text{ cm}^{-1}$ , and one at  $1260\text{ cm}^{-1}$  (deformation vibration  $\text{CH}_2$ ).<sup>16</sup> Comparison of this spectrum with that of pPAN shows clearly that the characteristic peak corresponding to  $\text{C}\equiv\text{N}$  has a split showing two peaks at  $2220$  and  $2250\text{ cm}^{-1}$ . Similarly the peak corresponding to  $\text{C}=\text{N}$  shifted to  $1640\text{ cm}^{-1}$  and appreciably broadened. The peak at  $1460\text{ cm}^{-1}$  does not show any shift but broadening is apparent. The peaks at  $1360$  and  $1260\text{ cm}^{-1}$  have greatly reduced intensity. It is noteworthy that a broad absorption in the region of  $3200-3500\text{ cm}^{-1}$  increased in intensity. This absorption occurs mainly due to  $\text{N}-\text{H}$  stretching. The intensity as well as width shows that

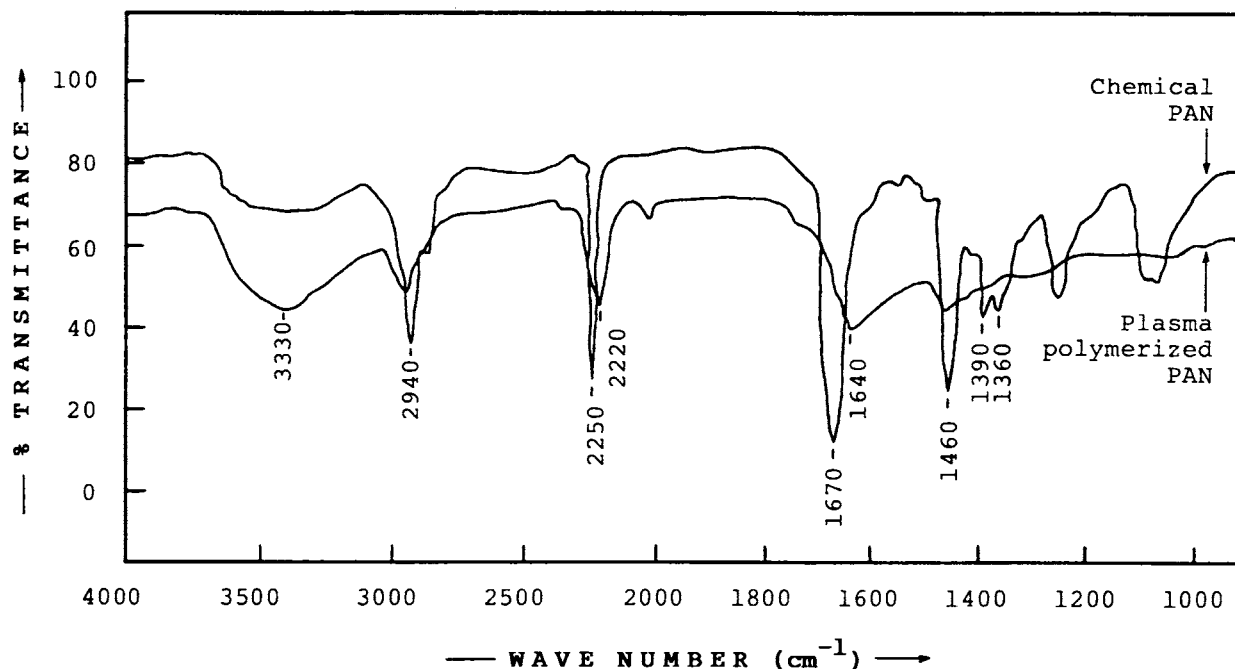


**Figure 6** IR spectra of chemically polymerized acrylonitrile (AN) and plasma polymerized AN films.

the plasma polymerized product contains nitrogen in several forms, particularly in the amide groups. The observation of the additional absorption band at  $2220\text{ cm}^{-1}$ , together with the peak at  $2250\text{ cm}^{-1}$  shows that  $\text{C}\equiv\text{N}$  moieties are intramolecularly bonded in the structure. This can arise because of higher cross-linking. Such splitting of the peak at 2250 and  $2230\text{ cm}^{-1}$  has been reported<sup>16</sup> and assigned to  $\text{C}\equiv\text{N}$  conjugated  $\text{C}=\text{N}$ , whereas the band at  $2030\text{ cm}^{-1}$  is assigned to ketone-imine ( $-\text{C}=\text{C}=\text{N}$ ) groups.<sup>17</sup> The ketone-imine group is more likely to be formed at low rf powers. We have indeed observed this band around  $2030\text{ cm}^{-1}$  for pPAN. In the plasma state dehydrogenation takes place and the hydrogen thus produced reduces the cyano group ( $\text{C}\equiv\text{N}$ ) into an amino group. In addition, radical formation takes place on the carbon atom in the backbone giving rise to chain growth that together with the interaction with the nitrile ( $\text{C}\equiv\text{N}$ ) group produces rapid cross-linking.

This reveals that the plasma polymerization of AN is complete and we do get polyacrylonitrile closely resembling commercial PAN.

## SOLUBILITY AND MOLECULAR WEIGHT

The pPAN formed was further characterized by testing its solubility in dimethylformamide (DMF) at room temperature. It was found that only 50% of the material dissolved. The remaining part was found to be insoluble even at  $150^\circ\text{C}$ , the boiling point of DMF. This could possibly be due either to a completely new type of material being formed in the plasma conditions or due to the very high molecular weight of the material. The molecular weight of the sample was, therefore, determined using gel permeation chromatography. However, the molecular weight of only the soluble component could be determined, which was found to be 185,000. On the other hand the molecular weight of conventionally polymerized PAN was 120,000. This shows that during the plasma polymerization rapid chain growth occurs giving rise to high molecular weight.

These longer chains in turn get highly cross-linked under the large dose of radiation and the UV components of the plasma. It is quite possible that very high cross-linking makes the material insoluble.

This work was carried out with the financial support of the Department of Science and Technology, Newer Fibres and Composites, New Delhi, India.

## REFERENCES

1. D. R. McKenzie and R. C. McPhedran, *Thin Solid Film*, **108**, 247 (1983).
2. N. Morosoff, W. Newton, and H. Yasuda, *J. Vac. Sci. & Technol.*, **15**, 1815 (1978).
3. N. Morosoff and H. Yasuda, *J. Vac. Sci. & Technol.*, **23**, 3471 (1979).
4. N. Morosoff and H. Yasuda, *ACS Symp. Ser.*, **108**, 163 (1979).
5. A. H. Bhuiyan and S. V. Bhorskar, *J. Mat. Sci.*, **24**, 3091 (1989).
6. N. Inagaki, S. Tasaka, and Y. Yamada, *J. Polym. Sci. A, Polym. Chem.*, **30**, 20003 (1992).
7. A. K. Sharma and H. Yasuda, *Thin Solid Films*, **110**, 171 (1985).
8. K. Kagganowicz and P. Datta, *Proc. Intern. Symp. Plasma Chem. Zurich*, 152 (1979).
9. H. Yasuda, *Plasma Polymerization*, Academic Press, Orlando, FL (1985).
10. Tadaaki Hirai and Osamu Nakadu, *Jap. J. Appl. Phys.*, **7**(2), 112 (1968).
11. J. L. Jacquemin and A. Ardalan, *J. Noncryst. Solids*, **28**, 249 (1978).
12. G. Brodure and J. L. Jacquemin, *J. Noncryst. Solids*, **50**, 389 (1982).
13. H. Yasuda and C. R. Wang, *J. Polym. Sci., Polym. Chem.*, **23**, 87 (1985).
14. M. Suzuki, K. Takahashi, and S. Mitani, *Jap. J. Appl. Phys.*, **14**, 741 (1975).
15. A. Bradley, *J. Electrochem. Soc.*, **119**, 1153 (1972).
16. S. I. Ivanov, *Eur. Polym. J.*, **20**, 415 (1984).
17. R. Liepins, D. Campbell, and C. Walker, *J. Polym. Sci., A-1*, **6**, 3059 (1968).

Received May 19, 1993

Accepted February 10, 1994